NIH Public Access
Author Manuscript
Neuroimage. Author manuscript; available in PMC 2015 January 15.

Published in final edited form as:
Neuroimage. 2014 January 15; 85(0 1): . doi:10.1016/j.neuroimage.2013.06.054.

Reducing motion artifacts for long-term clinical NIRS monitoring using collodion-fixed prism-based optical fibers

Meryem A. Yücel[1], **Juliette Selb**[1], **David A. Boas**[1], **Sydney S. Cash**[2], and **Robert J. Cooper**[1,3]

[1]HMS/MIT/MGH Athinoula A. Martinos Center for Biomedical Imaging, Department of Radiology, Massachusetts General Hospital, Harvard Medical School, Charlestown, MA, USA

[2]Neurology Department, Massachusetts General Hospital, Wang 720, Boston, MA, USA

[3]Department of Medical Physiology and Bioengineering, University College London, London, UK

Abstract

As the applications of near-infrared spectroscopy (NIRS) continue to broaden and long-term clinical monitoring becomes more common, minimizing signal artifacts due to patient movement becomes more pressing. This is particularly true in applications where clinically and physiologically interesting events are intrinsically linked to patient movement, as is the case in the study of epileptic seizures. In this study, we apply an approach common in the application of EEG electrodes to the application of specialized NIRS optical fibers. The method provides improved optode-scalp coupling through the use of miniaturized optical fiber tips fixed to the scalp using collodion, a clinical adhesive. We investigate and quantify the performance of this new method in minimizing motion artifacts in healthy subjects, and apply the technique to allow continuous NIRS monitoring throughout epileptic seizures in two epileptic in-patients. Using collodion-fixed fibers reduces the percent signal change of motion artifacts by 90 % and increases the SNR by 6 and 3 fold at 690 and 830 nm wavelengths respectively when compared to a standard Velcro-based array of optical fibers. The change in both HbO and HbR during motion artifacts is found to be statistically lower for the collodion-fixed fiber probe. The collodion-fixed optical fiber approach has also allowed us to obtain good quality NIRS recording of three epileptic seizures in two patients despite excessive motion in each case.

Keywords

Near-Infra Red Spectroscopy; Motion Artifact; Epilepsy

INTRODUCTION

Near-Infra Red Spectroscopy (NIRS) uses changes in the intensity of near-infrared light measured between source and detector optical fibers (‘optodes’) positioned on the head to

© 2013 Elsevier Inc. All rights reserved.

CONFLICT OF INTEREST

DB is an inventor on a technology licensed to TechEn, a company whose medical pursuits focus on noninvasive optical brain monitoring. DB’s interests were reviewed and are managed by Massachusetts General Hospital and Partners HealthCare in accordance with their conflict of interest policies.

Publisher's Disclaimer: This is a PDF file of an unedited manuscript that has been accepted for publication. As a service to our customers we are providing this early version of the manuscript. The manuscript will undergo copyediting, typesetting, and review of the resulting proof before it is published in its final citable form. Please note that during the production process errors may be discovered which could affect the content, and all legal disclaimers that apply to the journal pertain.

NIH-PA Author Manuscript

NIH-PA Author Manuscript

NIH-PA Author Manuscript

NIH-PA Author Manuscript

NIH-PA Author Manuscript

NIH-PA Author Manuscript

infer changes in hemoglobin concentrations in the cerebral cortex. The technique was first described by Jöbsis, (1977) and is increasingly used as a practical and inexpensive approach to investigating brain function in both clinical and research environments. NIRS has been used in a broad range of studies of healthy brain function (Obrig et al., 2002; White et al., 2010; Lloyd-Fox et al., 2010; Homae et al., 2011) and a wide spectrum of neurological diseases (Vernieri et al., 1999; Watanabe et al., 2002; Hock et al., 1997; Sakatani et al., 1999; Okada et al., 1994) (for a review: Irani et al., 2006).

One of the challenges of the application of NIRS is the occurrence of movement-induced artifacts. The NIRS signal is susceptible to motion artifacts because of relative movement between an optical fiber and the scalp. Optical contact can be temporarily or permanently altered due to this relative movement, which often occurs if the subject moves their head or face (Sweeney et al., 2011). Changes in optical contact result in pronounced artifact in the NIRS signal, and the amplitude of these motion artifacts is generally an order of magnitude larger than any underlying hemodynamic variations. This makes it very challenging to recover the actual physiological NIRS signal when measurement is contaminated by motion artifacts (Cooper et al., 2012a).

A major advantage of NIRS over techniques such as fMRI or PET is that NIRS is portable, and is therefore easily applied to vulnerable subject groups, such as infants, children or patients with neurological conditions. However, these groups are also much more likely to exhibit frequent movement and therefore produce motion artifacts. Epilepsy is one area of NIRS research that shows a lot of potential, as NIRS is one of the few techniques that can be used continuously and safely throughout epileptic seizures themselves. NIRS has been used in multiple studies of seizures in both infants and adults (Watanabe et al., 2002; Gallagher et al., 2008; Roche-Labarbe 2008; Cooper at al., 2011), and recent advances in data acquisition, processing and interpretation of NIRS data are likely to allow whole-head imaging of the hemodynamic and metabolic changes occurring in the cerebral cortex during seizures in the near future (Lareau et al., 2011; Takeuchi et al., 2009; Cooper et al., 2012b; Franceschini et al., 2006; Koch et al., 2010). However, epileptic seizures routinely involve excessive and often violent convulsions and movement of the head, and motion artifacts present a major obstacle to obtaining meaningful neurophysiological information about epileptic seizures.

Motion artifacts can be identified after measurements have been obtained, and there are various motion artifact removal techniques that can be applied to the signal (Robertson, 2010; Cooper, 2012). There are fundamentally two approaches to the minimization of motion artifacts: methods which require some external measurement of the movements of the subject (such as adaptive filtering (Zhang et al., 2007; Robertson 2010)) and methods that do not require extra measurements (such as principal component analysis, Kalman filtering, wavelet based filtering and spline interpolation (Zhang et al., 2005; Izzetoglu et al., 2010; Molavi et al., 2012; Scholkmann et al, 2012).

Methods of the first category use a measurement that is highly correlated to subject motion (such as an accelerometer signal) to inform a filtering algorithm of NIRS components that are likely to be artifact, which allows their removal in post-processing. The second category of motion artifact removal techniques uses some inherent characteristic of motion artifacts to remove them from the data. Applying principal component analysis (Zhang 2005), for example, relies on the assumption that motion artifacts provide a great majority of the variance of a given NIRS signal and that motion artifacts are apparent in multiple channels. Wavelet based filtering (Molavi et al., 2012) transforms the data into the wavelet domain and assumes that the outlying wavelet coefficients will be due to motion artifacts and these are removed from the data prior to performing the inverse wavelet transform.

NIH-PA Author Manuscript

NIH-PA Author Manuscript

NIH-PA Author Manuscript

Although these motion correction methods have been shown to be very effective in improving motion-contaminated data (Cooper et al., 2012), they cannot be as effective as simply avoiding the motion artifact in the first place. Because motion artifacts are due to relative motion between an optode and the scalp, providing stronger and more robust optode-scalp coupling can greatly improve the quality of NIRS data. Different techniques of applying optodes to head have been developed in order to optimize the NIRS signal with respect to factors such as hair, skin color, and fiber stability (Strangman et al., 2002). For example, brush optodes have been designed that improve the optical signal by threading through the hair (Khan et al., 2012). Another approach is to use a mechanical mounting structure to carry the weight of the optodes (Coyle et al., 2007; Giacometti and Diamond, 2013). Modified cycle helmets, thermoplastic moulded to the contours of each subject's head, spring-loaded fibers attached to semi-rigid plastic forms and fibers embedded in rubber forms are other alternative approaches of applying optodes to head (Strangman et al., 2002; Lloyd-Fox et al., 2010). In this study, we introduce a new way of applying NIRS optodes to the scalp which will reduce motion artifact contamination, as well as allow better optode-scalp contact and fiber stability against head. This will facilitate the use of NIRS in population groups where motion artifact contamination of the data is more likely. With this motivation, we designed a miniaturized optode, which allows the optical fiber tip to be fixed on the head using the same clinical adhesive that is commonly used to apply EEG electrodes for long term monitoring of epilepsy patients. We compare the efficacy of the new collodion-fixed fiber probe with a standard Velcro-based probe in a study of healthy subjects who simulated motions that capture the types of motions during a seizure. The new probe method was also applied to epilepsy in-patients in a clinical setting to allow long-term simultaneous NIRS and EEG monitoring. This study provided a further assessment of the utility of the new probe as it allowed us to obtain measurements of cerebral hemodynamics during seizures despite significant motion of the patient in each case.

METHODS

We have designed a miniaturized optical fiber tip (Figure 1) which consists of a glass prism (Casmed, Connecticut), a mirrored surface and a prism-housing that holds the prism and connects it to the optical fiber. The small size and low profile of this design means that it can be coupled to the head using a clinical adhesive (Collodion, Mavidon, FL), which is commonly used to apply EEG electrodes to the scalp. The application process is as follows. A towel is placed around the subject's shoulders in order to protect their clothing from the glue. The hair is parted using a cotton-tipped stick. A square of collodion-impregnated gauze (2–3 cm) is placed on the scalp as to cover the optode. The collodion is dried using compressed air.

Motion Artifact Study

To provide a quantified assessment of the efficacy of the collodion-fixed optical fibers, we performed a study which applied both collodion-fixed and standard optical fiber probes to healthy subjects. Five healthy adult subjects were recruited for this study (1 female, 4 male). The subjects were 23–52 years old (mean 35 ± 13). The study was approved by Massachusetts General Hospital and each subject gave informed written consent.

Data were collected using a TechEn CW6 system operating at 690 and 830 nm (TechEn Inc. MA, USA). The standard Velcro-based NIRS probe contained 2 sources and 4 detectors and was located over the right motor region of each subject. The collodion-fixed fibers were attached over the left hemisphere of the subject so as to symmetrically match the standard probe (Fig. 2). Fig. 2 and 3 are obtained using Atlasviewer, part of the HOMER2 NIRS processing package (Huppert et al., 2009). The 3D positions of the sources and detectors are obtained using a 3D digitizer (Polhemus, VT). During recording, subjects were asked to

NIH-PA Author Manuscript

NIH-PA Author Manuscript

NIH-PA Author Manuscript

perform seven different types of movement in order to induce motion artifacts mimicking normal motions as well as motions seen during seizure: reading aloud, nodding their head up and down, nodding sideways, twisting right, twisting left, shaking head rapidly from side to side and raising their eyebrows. The Psychophysics toolbox for Matlab (Brainard, 1997) was used to control the timing of the experiment. Each motion trial was performed for 3 seconds and trials were repeated 5 times for each motion type with a randomized inter-trial interval of between 5 and 10 seconds. This resulted in a 6 minute-long recording period. Following this, we acquired 12 minutes of resting state data, with the same probe arrangement.

Epilepsy Study

As part of an ongoing clinical study, we have begun to apply collodion-fixed optical fibers to epilepsy in-patients. The subjects were recruited from the in-patients of the Epilepsy Monitoring Unit of Massachusetts General Hospital (Table 1). The Massachusetts General Hospital Institutional Review Board approved the study and all subjects gave informed written consent which included the application of collodion. Our optical probes were fixed to the head at the same time as the clinical EEG electrodes so as to minimize the impact of our study to the standard clinical procedure.

The positioning of the optical probes was decided based on the medical history of patient, so as to maximize the likelihood that NIRS measurements would be sensitive to the epileptic focus (Fig. 3). The EEG electrodes are placed according to the clinically standard International 10–20 system (XLTEK a division of Natus, Ontario, Canada). The optical fibers used in this study were ~11 m in length, allowing the subjects to move comfortably about their room and use the restroom.

Data Analysis

Motion Artifact Study—We have used four metrics to compare the quality of the signal from the collodion-fixed fiber probe and the Velcro-based probe. The first metric is the group average of signal to noise ratio of light intensity for each probe type. Signal to noise ratio is calculated as the ratio of the mean over the standard deviation of the raw signal i.e. unfiltered light intensity at each wavelength. We did not do any preprocessing prior to this. Our second measure is the percent signal change in light intensity during motion artifact. The percent signal change from baseline during motion artifact is obtained as the ratio of the raw signal averaged from 0 to 4 seconds after the purposefully induced motion artifact to the raw signal averaged from −4 to 0 seconds prior to motion artifact for each stimulus type separately (Eq. 1).

$$\%SignalChange = 100 \times \left[1 - \frac{[Signal]_{Motion\ Artifact\ [0\ to\ 4sec]}}{[Signal]_{Baseling\ [-4\ to\ 0\ sec]}} \right] \quad \text{(Eq. 1)}$$

As a third metric we calculated the group average of the standard deviation of changes in oxyhemogolobin (HbO) and deoxyhemoglobin (HbR) concentrations calculated over the length of each data set as well as the changes in HbO and HbR during each motion artifact case. For this calculation, the raw NIRS signal was first converted into changes in optical density by taking the logarithm of the signal. The changes in HbO and HbR concentrations were then obtained using the Beer-Lambert law with a partial pathlength factor of 6 (Cope and Deply, 1998; Deply et al., 1988; Boas et al., 2004). To obtain the changes in HbO and HbR during each motion artifact type, we averaged from 0 to 4 seconds after the purposefully induced motion artifact.

NIH-PA Author Manuscript

NIH-PA Author Manuscript

NIH-PA Author Manuscript

Our last metric was the cardiac signal to noise ratio during rest. A good fNIRS signal will clearly show fluctuations arising from systemic physiology. In particular, visualization of the cardiac pulse is an indication of good coupling of the optodes on the scalp. For this reason, a traditional measure of SNR defined as the ratio of the signal mean over its standard deviation can be misleading, as high fluctuations at the cardiac frequency will result in high standard deviation and be interpreted as a noisy signal. Inversely, high SNR could be artificially achieved if a high signal level without physiological fluctuations is detected because the light does not actually travel in the head. Therefore, in addition to the traditional SNR metric obtained during motion artifact runs, we calculated a cardiac signal to noise ratio during rest defined as the ratio of the power in the cardiac frequency band (0.8 to 1.67Hz) over the noise power in the high frequency range (5Hz to 20Hz), expressed on a logarithmic scale. The power spectral density of the resting state data is estimated using Welch's method for the above calculation (Welch, 1967).

Epilepsy Study—The NIRS signals from each epilepsy patient were first converted to changes in optical density and then to changes in HbO and HbR concentrations using Beer's Lambert law with a partial pathlength factor of 6 (Cope and Deply, 1998; Deply et al., 1988; Boas et al., 2004). We did not make any partial volume correction assuming the seizure results in a global response rather than local.

By assuming a baseline total hemoglobin concentration of 60 μM (Torricelli et al., 2001), we calculated the relative changes in total hemoglobin concentration (rtHb) and used this to substitute for relative cerebral blood volume (rCBV), since they are equal under a constant hematocrit assumption (Siegel et al., 2003). We then used the Grubb relation (Grubb et al., 1974) to obtain the relative cerebral blood flow (rCBF) from rCBV. The cerebral metabolic rate of oxygen relative to baseline ($rCMRO_2$) can then be calculated as the product of the relative oxygen extraction fraction (rOEF) and rCBF (Hoge et al., 2005). $CMRO_{2,0}$, OEF_0, CBF_0, HbR_0 and tHb_0 are the baseline values for these variables.

$$rCMRO_2 = \frac{CMRO_2}{CMRO_{2,0}} = \frac{OEF}{OEF_0}\frac{CBF}{CBF_0} \quad \text{(Eq. 2)}$$

OEF is obtained using the following equation, assuming a baseline oxygen extraction fraction of 0.4 (Raichle et al., 2001).

$$OEF = OEF_0 \cdot \frac{[HbR]}{[HbR]_0}\frac{[tHb]_0}{[tHb]} \quad \text{(Eq. 3)}$$

The EEG recordings were acquired at a sampling rate of 256 Hz. The data were bandpass filtered at 0.3–20 Hz using a fifth order Butterworth filtering. The EEG traces were transformed into a bipolar representation.

RESULTS

Assessment in Healthy Volunteers

An example of the unfiltered light intensity at 690 nm wavelength from a symmetrically located pair of NIRS channels, one collodion-fixed and one Velcro-fixed is shown in Fig. 4 where the subject mimics normal as well as seizure-born motion. Results are shown for the whole run in Fig. 4A, and for individual motion artifacts in Fig. 4B, C, D and E. The subject movement produces noticeably smaller amplitude artifacts in the signal recorded using the collodion-fixed probe. An example of a motion-induced shift in baseline signal is shown in

NIH-PA Author Manuscript

NIH-PA Author Manuscript

NIH-PA Author Manuscript

Fig. 4C. While the shift is maintained even after the movement at the Velcro probe side, the signal level is recovered at the collodion-fixed fiber probe side.

The signal to noise ratio (SNR) was computed for both the signal recorded at collodion-fixed fiber probe and Velcro probe sides at 690 and 830 nm wavelengths. Fig. 5 shows the SNR averaged over 5 subjects. The means and the standard deviations of SNR for the collodion-fixed and Velcro probe are 28.64 ± 13.71 and 4.3 ± 2.78 at 690 nm wavelength and 27.24 ± 9.54 and 7.24 ± 5.24 at 830 nm wavelength respectively. Collodion-fixed probes result in significantly higher SNR values compared to the Velcro probe at both wavelengths (paired t-test, $p<0.001$). The right panel in Fig. 5 shows the standard deviation of changes in HbO and HbR calculated over the length of each data set, averaged over all subjects. The mean and standard deviation of standard deviation for collodion-fixed fiber probe and Velcro probe are 0.6 ± 0.2 and 3.1 ± 1.4 μM for HbO and 0.3 ± 0.2 and 2.1 ± 1.2 μM for HbR respectively. The averaged standard deviation for Collodion-fixed fiber probe is statistically lower than that of Velcro probe (paired t-test, p-value<0.001).

The percent signal change from baseline as a response to each different movement averaged over all trials is shown in Fig. 6A for 690 nm and in Fig. 6B for 830 nm wavelengths (see Table 2 for median percent signal changes). The percent signal change is statistically lower in all motion artifact cases for the collodion-fixed probes for both wavelengths (paired t-test, p-value<0.001). The highest changes in signal were observed during eyebrow raising and nodding up and down (Fig. 6A and B). While the median percent signal change is always less than 3 % for the collodion-fixed fiber probe, it reaches 20 % for the Velcro probe. There is no significant difference between the cardiac signal to noise of the two groups (figure not shown).

Fig. 7 shows the changes in HbO and HbR during each induced movement, averaged over all trials. The median values for each movement type can be found in Table 3. The change in both HbO and HbR for each motion artifact type is statistically higher for the Velcro probe (paired t-test, p-value<0.001). The highest median values of changes in HbO and HbR are 4.1 and 2.2 μM which happens during raising eyebrows.

Epilepsy Study

Fig. 8 and 9 show data from a 36-year old male patient with epilepsy undergoing EEG-NIRS recording. This patient underwent 6 hours of continuous EEG-NIRS recording with 7 NIRS channels (Fig. 3, left), during which time he suffered two electro-clinical seizures (seizure 1: 114 sec long, seizure 2: 20 sec long) which were accompanied by severe convulsions. The EEG-NIRS data for a single NIRS channel is shown in Fig. 8 for the first seizure and in Fig. 9 for the second seizure. A large increase in HbO and tHb begins a few seconds prior to the onset of the EEG burst (Fig. 8 and 9). The rise in HbO and tHb in the first ten seconds of each seizure is followed by a return towards baseline in both cases. However, for seizure 1 HbO and tHb continue to decrease well below baseline, resulting in a period of deoxygenation which only begins to recover after the seizure ends. The increase in SNR at the end of seizure (at 114 s) is due to the cessation of the violent jerks which were occurring during the seizure as revealed by the video recordings. The slower shift in tHb and CBF that occur thereafter are related to the recovery of the hemodynamics from the seizure state. rCBF and $rCMRO_2$ show a peak increase of approximately 80 % and 60 % in the first seizure and 135 % and 100 % in the second seizure, and closely match each other throughout the majority of the duration of the seizure. They differ most significantly at their peak, where the ratio of $CBF/CMRO_2$ is at a maximum. The average value of this flow-consumption ratio at this peak across both seizures in this patient was ~1.15.

NIH-PA Author Manuscript

NIH-PA Author Manuscript

NIH-PA Author Manuscript

Fig. 10 shows a 59-year old female patient who was recorded for 18 hrs continuously with 4 NIRS channels symmetrically located at each hemisphere. During recording she underwent one electro-clinical seizure (Fig. 10 (seizure duration: 53 sec)). The rise in HbO and tHb concentrations lasted longer (40 sec) for this subject. Once again, the changes in CBF and $CMRO_2$ closely match one another- leading to a flow-demand ratio that has a maximum value of 1.1.

DISCUSSION

Motion artifacts, generally being orders of magnitude larger than physiological NIRS signals, can result in the loss of much useful data. In cases where severe movements occur during the physiological response of interest, such as in seizures, motion artifacts are a major problem. Although there are several algorithms that correct for motion artifacts, more direct solutions are desirable. In this study, we introduced a new method of attaching NIRS optical fibers to the scalp using a miniaturized optical fiber tip and the clinical adhesive that is routinely used for EEG electrodes. In the first part, measurements were taken from healthy volunteers who performed normal motions such as nodding, reading aloud, etc as well as motions that occur during seizure such as rapidly head shaking or twisting. The subjects had a regular Velcro probe on one side of their heads and collodion-fixed fiber probe on the other, to allow direct comparison. This study allowed us to compare the efficacy of the two probes. The collodion-fixed fiber probe was shown to be significantly less susceptible to motion artifacts than the standard Velcro probe using all the metrics we calculated. The second part of the study involved measurements of epilepsy inpatients during seizures. These patients had only collodion-fixed fiber probes, since the Velcro probe is incompatible with the long-term, clinical EEG paradigm. Although a direct comparison between the performance of the Velcro and collodion-fixed probes cannot be performed in these patients, the quality of the NIRS data obtained during seizures suggests that the improvement provided by the collodion-fixed fibers is as good or better than for the healthy subjects. It is important to note that the video recordings of the epilepsy patients reveal that in each case, the patient's motions are much more extreme than the motions performed by the healthy volunteers.

Collodion is a water-resistant adhesive and is easy to apply and remove, but it has some disadvantages. Ethyl ether and ethanol in collodion evaporate during application and leave an adhesive film of nitrocellulose. The fumes emitted by collodion can cause irritation of the nose and eyes. However it has been shown that these risks can be minimized by proper ventilation (Young et al., 1993). As a result, collodion has been routinely used for securing electrodes in EEG laboratories throughout the world since the 1970s. Moreover, since the collodion impregnated gauze is relatively opaque, completely covers each fiber and holds it tightly to the skin, it will minimize the chance of light travelling from source to detector without travelling through the tissue of the head.

The results from our study of healthy volunteers show a dramatic reduction of motion artifacts using the new collodion-fixed fiber probe as compared to regular Velcro probe. The SNR was statistically higher and the percentage signal change resulting from motion was significantly lower for the collodion-fixed probe. The largest amplitude motion artifacts occurred in response to raising the eyebrows followed by nodding the head up and down. It is likely that these movements cause the largest movement of the scalp relative to NIRS optodes. The changes in HbO and HbR were statistically higher for Velcro probe. The values were comparable to values obtained during an actual functional hemodynamic response (eg 4.1 μM) (Obrig et al., 2002). In contrast, the changes were no more than 0.5 μM for the collodion-fixed probe, which suggests that the collodion-fixed probe may reduce

NIH-PA Author Manuscript

NIH-PA Author Manuscript

NIH-PA Author Manuscript

motion artifacts to the point where they are significantly smaller than the signal of interest, i.e. the functional hemodynamic response.

To provide a measure of the physiological content of the NIRS signals, we also compared the cardiac signal to noise of the NIRS data obtained using each probe type during rest. There was no significant difference between the cardiac signal to noise of each probe type which shows that the coupling is similar for each probe, however the collodion-fixed fiber probe is superior during motion artifacts.

A potential limitation of this study was that the position of the collodion-fixed fibers on the head was not randomized between right and left, and there is a small possibility that asymmetric subject motion may have introduced a bias. We tried to avoid any potential bias in the motions themselves by including bilateral movements such as nodding right and nodding left.

Our EEG-NIRS study of epileptic in-patients was only possible because of the miniaturized optical fiber design, which has allowed us to apply NIRS fibers using the same clinical adhesive used to apply EEG electrodes. The new probes allowed long-term recordings of epilepsy in-patients up to 24 hours. This has made it possible to capture multiple seizures in each patient using simultaneous EEG-NIRS recordings, which is not possible using other modalities such as MEG, fMRI or PET imaging.

The flow-consumption ratio is a relatively robust measure of neurovascular coupling (Boas et al., 2003). The ratios obtained were 1.1, 1.2 and 1.1 in the three seizures measured. These values are close to one, which is considerably lower than those seen in normal functional brain activity (Buxton, 2010). This is an indication of larger increases in $CMRO_2$ relative to blood flow during seizures than is normally seen during a functional response. This may indicate that the brain tissue affected by seizures may temporarily enter a hypoxic state that can potentially be damaging. The flow-consumption calculations are susceptible to errors due to the assumptions made in the calculation of $CMRO_2$ and CBF. Thus we performed a sensitivity analysis to determine the sensitivity of flow-consumption ratio across a physiologically feasible range of the assumed parameters. The flow-consumption ratio showed a maximum 10 % change when the baseline value, $tHb_{0,}$ was varied across the range of 60–140 μM and OEF was varied across the range of 0.2–0.45 (see Boas et al, 2003 for an examination of the physiological validity of these ranges). Another assumption we made was to apply the Grubb relation, which is a power law relating blood volume and blood flow. The range of the exponent is thought to be between 0.18–0.36 during functional activation (Boas et al., 2003). Our analysis showed that the flow-consumption ratio is fairly robust within this interval, exhibiting a maximum 2 % change. Including direct CBF measurements in future experiments (using, for example, diffuse correlation spectroscopy (Mesquita et al., 2011) would allow this assumption to be avoided.

Although this approach requires each optical fiber to be coupled to the head individually (rather than fixing an array of fibers in place), we have found the adhesive approach to be extremely beneficial. As shown by the results above, we were able to extract useful physiological measures of blood oxygenation and blood volume changes in epilepsy patients during seizures (Fig. 8, 9 and 10) despite those seizures being accompanied by severe convulsions. This was possible because the clinical adhesive ensures that there is little relative motion between the fiber tip and the scalp, which renders the NIRS channels insensitive to motion artifacts. This is vitally important, as it makes it much easier to obtain continuous NIRS recording throughout a clinical seizure. Moreover, the individual application of the optical fibers to the scalp means that we can ensure good optical contact; hair can be moved out from underneath the fiber tip. This maximizes the transmission of

NIH-PA Author Manuscript

NIH-PA Author Manuscript

NIH-PA Author Manuscript

light in an out of the tissue, which significantly improves the NIRS signal. In addition, this approach is no more difficult or time consuming than the application of standard EEG electrodes and is just as comfortable and safe for the patient. One important issue that is not addressed by the probe design described here is the effect on the NIRS signal of head-tilting, or changes in the position of the head relative to the heart. Seizures often result in patients leaning or turning in a particular direction, which, as well as causing transient motion artifacts like those addressed here, causes the cerebral blood volume to change due to gravity. These signals cannot be minimized by improved fiber coupling, but as they are likely to be slow and affect multiple channels and be apparent in scalp tissues, it is likely they could be minimized by a process of regression (see Gagnon et al., 2011).

Overall our results show that collodion-fixed optical fibers provide a significant advantage over standard optical fiber coupling approaches. Collodion-fixed optical fibers may prove essential to the continued uptake of NIRS in clinical scenarios, particularly in the study of epileptic seizures.

CONCLUSION

In this study, we have introduced a method of attaching optodes to head using miniaturized optical fiber tips and a standard clinical adhesive. These collodion-fixed probes are superior to regular Velcro-based probes in terms of the signal-to-noise ratio they can achieve and the reduction in the percent signal change during motion artifacts. The collodion-fixed probes reduce the maximum signal change due to motion artifacts from 103 % (Velcro probe) to 9 % (Fig. 6) and have the potential to enable robust, long-term NIRS recordings in subjects and patients who have limited or transient motor control.

Acknowledgments

This work was supported by NIH grants P41-RR14075, R01-EB006385 and R90-DA023427. We would like to thank Andres Salom, Kara Houghton and Kristy Nordstrom at the Epilepsy Monitoring Unit of Massachusetts General Hospital and Sabrina Brigadoi at Martinos Center for Biomedical Imaging for all their help.

References

Boas DA, Strangman G, Culver JP, Hoge RD, Jasdzewski G, Poldrack RA, Rosen BR, Mandeville JB. Can the cerebral metabolic rate of oxygen be estimated with near-infrared spectroscopy? Phys Med Biol. 2003; 48(15):2405–18. [PubMed: 12953906]

Boas D, Dale AM, Franceschini MA. Diffuse optical imaging of brain activation: Approaches to optimizing image sensitivity, resolution and accuracy. Neuroimage. 2004; 23:S275–S288. [PubMed: 15501097]

Brainard DH. The psychophysics toolbox. Spatial Vision. 1997; 10:433–436. [PubMed: 9176952]

Buxton RB. Interpreting oxygenation-based neuroimaging signals: the importance and the challenge of understanding brain oxygen metabolism. Front Neuroenergetics. 2010 Jun.17:2, 8.

Cooper RJ, Hebden JC, O'Reilly H, Mitra S, Michell AW, Everdell N, Gibson AP, Austin T. Transient Haemodynamic Events in Neurologically Compromised Infants: A Simultaneous EEG and Diffuse Optical Imaging Study. NeuroImage. 2011; 55(4):1610–616. [PubMed: 21255658]

Cooper RJ, Caffini M, Dubb J, Fang Q, Custo A, Tsuzuki D, Fischl B, Wells W III, Dan I, Boas DA. Validating atlas-guided DOT: A comparison of diffuse optical tomography informed by atlas and subject-specific anatomies. Neuroimage. 2012a; 62(3):1999–2006. [PubMed: 22634215]

Cooper RJ, Selb J, Gagnon L, Phillip D, Schytz HW, Iversen HK, Ashina M, Boas DA. A systematic comparison of motion artifact correction techniques for functional near-infrared spectroscopy. Front Neurosci. 2012b; 6:147. [PubMed: 23087603]

NIH-PA Author Manuscript

NIH-PA Author Manuscript

NIH-PA Author Manuscript

Cope M, Deply DT. System for long-term measurement of cerebral blood flow and tissue oxygenation on newborn infants by infrared transillumination. Med Biol Eng Comput. 1998; 26:289–294. [PubMed: 2855531]

Coyle SM, Ward TE, Markham CM. Brain-computer interface using a simplified functional near-infrared spectroscopy system. J Neural Eng. 2007; 4(3):219–26. [PubMed: 17873424]

Deply DT, Cope M, van der Zee P, Arridge S, Wray S, Wyatt J. Estimation of optical pathlength through tissue from direct time of light measurement. Phys Med Biol. 1988; 33:1433–1442. [PubMed: 3237772]

Franceschini MA, Joseph DK, Huppert TJ, Diamond SG, Boas DA. Diffuse Optical Imaging of the Whole Head. Journal of Biomedical Optics. 2006; 11(5):054007. [PubMed: 17092156]

Gallagher A, Lassonde M, Bastien D, Vannasing P, Lesage F, Grova C, Bouthillier A, Carmant L, Lepore F, Béland R, Nguyen DK. Non-invasive pre-surgical investigation of a 10 year-old epileptic boy using simultaneous EEG-NIRS. Seizure. 2008; 17(6):576–82. [PubMed: 18374608]

Gagnon L, Perdue K, Greve DN, Goldenholz D, Kaskhedikar G, Boas DA. Improved recovery of the hemodynamic response in diffuse optical imaging using short optode separations and state-space modeling. Neuroimage. 2011; 56(3):1362–1371. [PubMed: 21385616]

Giacometti P, Diamond SG. Compliant head probe for positioning electroencephalography electrodes and near-infrared spectroscopy optodes. J Biomed Opt. 2013; 18(2):27005. [PubMed: 23377012]

Grubb RL, Raichle ME, Eichling JO, Ter-Pogossian MM. The Effects of Changes in PaCO2 on Cerebral Blood Volume, Blood Flow, and Vascular Mean Transit Time Stroke. 1974; 5(5):630–9.

Hock C, Villringer K, Muller-Spahn F, Hofmann M, Schuh-Hofer S, Heekeren H, Wenzel R, Dirnagl U, Villringer A. Near infrared spectroscopy in the diagnosis of Alzheimer's disease. Annals of the New York Academy of Sciences. 1996; 777:22–29. [PubMed: 8624087]

Hoge RD, Franceschini MA, Covolan RJ, Huppert T, Mandeville JB, Boas DA. Simultaneous recording of task-induced changes in blood oxygenation, volume, and flow using diffuse optical imaging and arterial spin-labeling MRI. Neuroimage. 2005; 25(3):701–7. [PubMed: 15808971]

Homae F, Watanabe H, Nakano T, Taga G. Large-scale brain networks underlying language acquisition in early infancy. Front Psychol 2011. 2011; 2:93.

Huppert TJ, Diamond SG, Franceschini MA, Boas DA. HomER: a review of time-series analysis methods for near-infrared spectroscopy of the brain. Appl Opt. 2009; 48(10):D280–98. [PubMed: 19340120]

Irani F, Platek SM, Bunce S, Ruocco AC, Chute D. Functional near infrared spectroscopy (fNIRS): an emerging neuroimaging technology with important applications for the study of brain disorders. Clin Neuropsychol. 2007; 21(1):9–37. [PubMed: 17366276]

Izzetoglu M, Chitrapu P, Bunce S, Onaral B. Motion artifact cancellation in NIR spectroscopy using discrete Kalman filtering. Biomed Eng Online. 2010; 9;9:16.

Jobsis FF. Noninvasive infrared monitoring of cerebral and myocardial sufficiency and circulatory parameters. Science. 1977; 198(4323):1264–7. [PubMed: 929199]

Khan B, Wildey C, Francis R, Tian F, Delgado MR, Liu H, Macfarlane D, Alexandrakis G. Improving optical contact for functional near-infrared brain spectroscopy and imaging with brush optodes. Biomed Opt Express. 2012; 3(5):878–98. [PubMed: 22567582]

Koch SP, Habermehl C, Mehnert J, Schmitz CH, Holtze S, Villringer A, Steinbrink J, Obrig H. High-resolution optical functional mapping of the human somatosensory cortex. Front Neuroenergetics. 2010; 2:12. [PubMed: 20616883]

Lareau E, Lesage F, Pouliot P, Nguyen D, Le Lan J, Sawan M. Multichannel wearable system dedicated for simultaneous electroencephalography/near-infrared spectroscopy real-time data acquisitions. J Biomed Opt. 2011; 16(9)

Lloyd-Fox S, Blasi A, Elwell CE. Illuminating the developing brain: the past, present and future of functional near infrared spectroscopy. Neurosci Biobehav Rev. 2010; 34(3):269–84. [PubMed: 19632270]

Mesquita RC, Durduran T, Yu G, Buckley EM, Kim MN, Zhou C, Choe R, Sunar U, Yodh AG. Direct measurement of tissue blood flow and metabolism with diffuse optics. Philos Transact A Math Phys Eng Sci. 2011; 369(1955):4390–406.

NIH-PA Author Manuscript

NIH-PA Author Manuscript

NIH-PA Author Manuscript

Molavi B, Dumont GA. Wavelet-based motion artifact removal for functional near-infrared spectroscopy. Physiol Meas. 2012; 33(2):259–70. [PubMed: 22273765]

Obrig H, Israel H, Kohl-Bareis M, Uludag K, Wenzel R, Müller B, Arnold G, Villringer A. Habituation of the visually evoked potential and its vascular response: implications for neurovascular coupling in the healthy adult. Neuroimage. 2002; 17(1):1–18. [PubMed: 12482064]

Okada F, Tokumitsu Y, Hoshi Y, Tamura M. Impaired interhemispheric integration in brain oxygenation and hemodynamics in schizophrenia. European Archives of Psychiatry and Clinical Neuroscience. 1994; 244(1):17–25. [PubMed: 7918697]

Raichle ME, MacLeod AM, Snyder AZ, Powers WJ, Gusnard DA, Shulman GL. A default mode of brain function. Proc Nat Acad Sci U S A. 2001; 98:676–682.

Robertson FC, Douglas TS, Meintjes EM. Motion artifact removal for functional near infrared spectroscopy: a comparison of methods. IEEE Trans Biomed Eng. 2010; 57(6):1377–87. [PubMed: 20172809]

Roche-Labarbe N, Zaaimi B, Berquin P, Nehlig A, Grebe R, Wallois F. NIRS-measured Oxy- and Deoxyhemoglobin Changes Associated with EEG Spike-and-wave Discharges in Children. Epilepsia. 2008; 49(11):1871–880. [PubMed: 18631367]

Sakatani K, Katayama Y, Yamamoto T, Suzuki S. Changes in cerebral blood oxygenation of the frontal lobe induced by direct electrical stimulation of thalamus and globus pallidus: A near infrared spectroscopy study. Journal of Neurology, Neurosurgery and Psychiatry. 1999; 67(6): 769–773.

Scholkmann F, Spichtig S, Muehlemann T, Wolf M. How to detect and reduce movement artifacts in near-infrared imaging using moving standard deviation and spline interpolation. Physiol Meas. 2010; 31(5):649–62. [PubMed: 20308772]

Siegel AM, Culver JP, Mandeville JB, Boas DA. Temporal comparison of functional brain imaging with diffuse optical tomography and fMRI during rat forepaw stimulation. Phys Med Biol. 2003; 48(10):1391–403. [PubMed: 12812454]

Strangman G, Boas DA, Sutton JP. Non-invasive neuroimaging using near-infrared light. Biol Psychiatry. 2002; 52(7):679–93. [PubMed: 12372658]

Sweeney KT, Ayaz H, Ward TE, Izzetoglu M, McLoone SF, Onaral BA. Methodology for Validating Artifact Removal Techniques for fNIRS. Conf Proc IEEE Eng Med Biol Soc. 2011:4943–6. [PubMed: 22255447]

Takeuchi M, Hori E, Takamoto K, Tran AH, Satoru K, Ishikawa A, Ono T, Endo S, Nishijo H. Brain cortical mapping by simultaneous recording of functional near infrared spectroscopy and electroencephalograms from the whole brain during right median nerve stimulation. Brain Topogr. 2009; 22:197–214. [PubMed: 19705276]

Torricelli A, Pifferi A, Taroni P, Giambattistelli E, Cubeddu R. In vivo optical characterization of human tissues from 610 to 1010 nm by time-resolved reflectance spectroscopy. Phys Med Biol. 2001; 46(8):2227–2237. [PubMed: 11512621]

Vernieri F, Rosato N, Pauri F, Tibuzzi F, Passarelli F, Rossini PM. Near infrared spectroscopy and transcranial Doppler in monohemispheric stroke. Eur Neurol. 1999; 41(3):159–62. [PubMed: 10202248]

Watanabe E, Nagahori Y, Mayanagi Y. Focus Diagnosis of Epilepsy Using Near-Infrared Spectroscopy. Epilepsia. 2002; 43:50–55. [PubMed: 12383281]

Welch PD. The Use of Fast Fourier Transform for the Estimation of Power Spectra: A Method Based on Time Averaging Over Short, Modified Periodograms. IEEE Trans Audio Electroacoustics. 1967; AU-15:70–73.

White BR, Culver JP. Quantitative evaluation of high-density diffuse optical tomography: in vivo resolution and mapping performance. J Biomed Opt. 2010; 15(2):026006. [PubMed: 20459251]

Young B, Blais R, Campbell V, Covacich D, Demelo J, Leitch G, MacKenzie J, Schieven J. Vapors from collodion and acetone in an EEG laboratory. J Clin Neurophysiol. 1993; 10(1):108–10. [PubMed: 8458989]

Zhang Y, Brooks DH, Franceschini MA, Boas DA. Eigenvector-based spatial filtering for reduction of physiological interference in diffuse optical imaging. J Biomed Opt. 2005; 10:11014. [PubMed: 15847580]

Zhang Q, Brown EN, Strangman GE. Adaptive filtering for global interference cancellation and real-time recovery of evoked brain activity: a Monte Carlo simulation study. J Biomed Opt. 2007; 12(4):044014. [PubMed: 17867818]

NIH-PA Author Manuscript

NIH-PA Author Manuscript

NIH-PA Author Manuscript

NIH-PA Author Manuscript

NIH-PA Author Manuscript

NIH-PA Author Manuscript

Research Highlights

The use of miniaturized optical fiber tips fixed to the scalp using collodion reduces motion artifact. Using collodion-fixed fibers reduces the percent signal change of motion artifacts by 90 %. The new method increases the SNR by 6 and 3 fold at 690 and 830 nm wavelengths respectively.

NIH-PA Author Manuscript

NIH-PA Author Manuscript

NIH-PA Author Manuscript

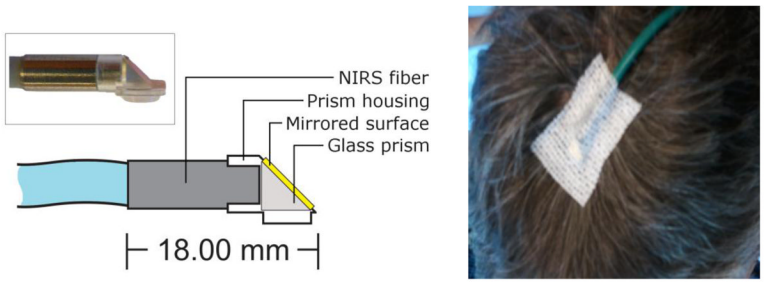

Fig. 1.
Diagram of prism-based fiber (left), collodion-fixed prism-based fiber with impregnated gauze on top (right)

NIH-PA Author Manuscript

NIH-PA Author Manuscript

NIH-PA Author Manuscript

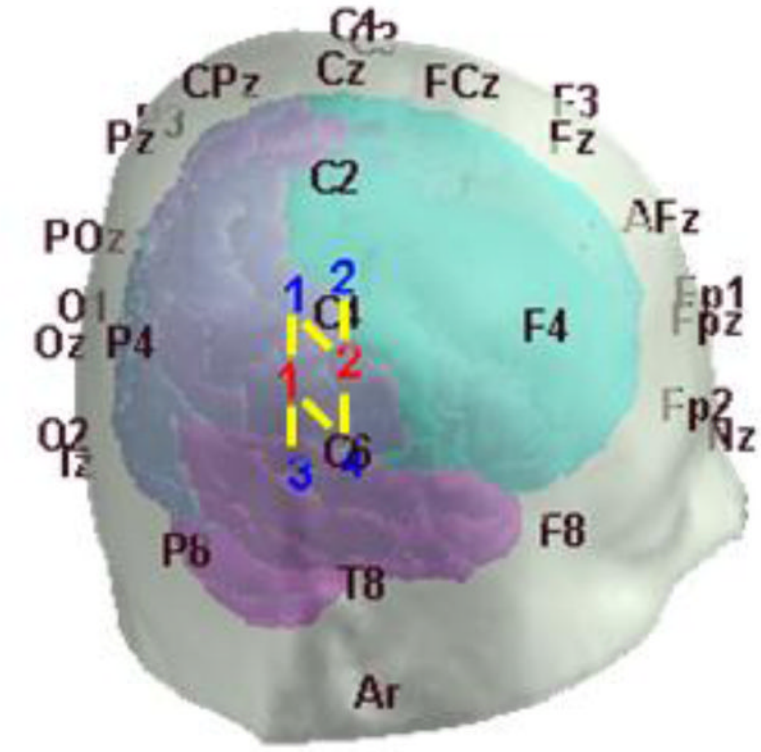

Fig. 2.
Optical probe for the motion artifact study. Symmetrical source detector localization on both hemispheres. The red and blue numbers indicate the position of sources and detectors respectively. The yellow lines indicate a source-detector pair, or channel.

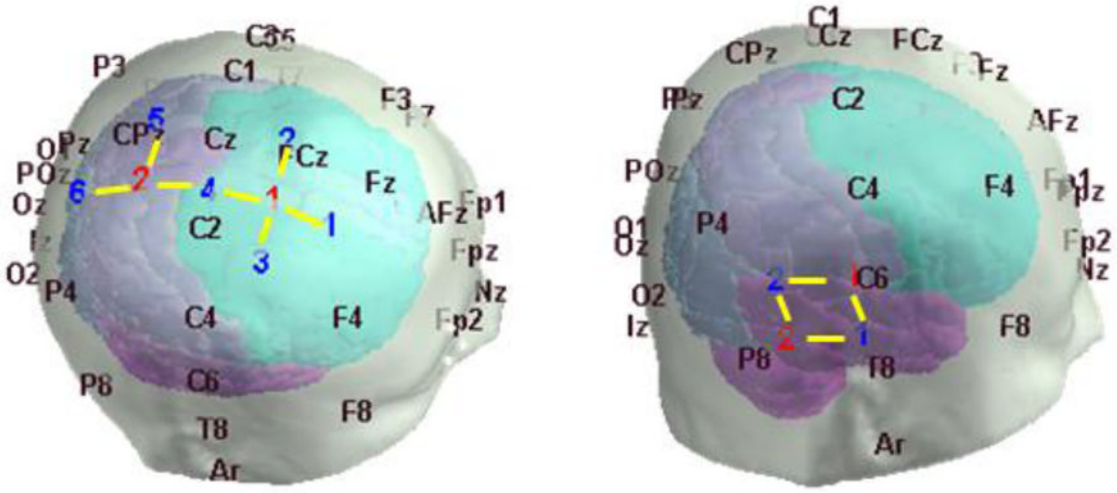

Fig. 3.

Probe arrangement in epilepsy patients for subject 1 (left, one side), subject 2 (right, symmetrical on both sides). The red and blue numbers indicate the position of sources and detectors respectively. The yellow lines indicate a source-detector pair, or channel.

NIH-PA Author Manuscript NIH-PA Author Manuscript NIH-PA Author Manuscript

NIH-PA Author Manuscript

NIH-PA Author Manuscript

NIH-PA Author Manuscript

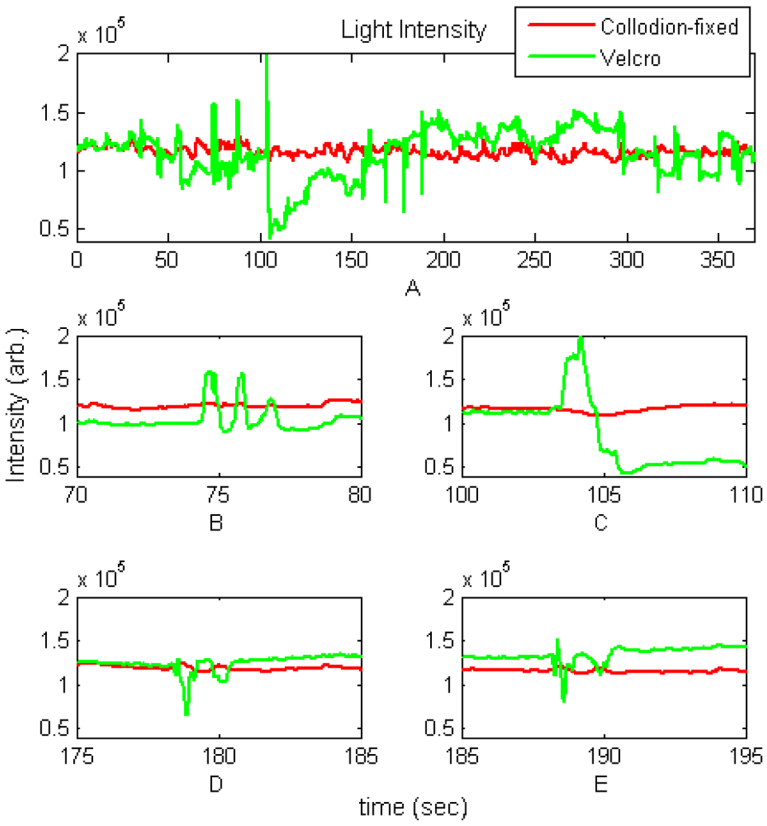

Fig. 4.

Raw NIRS signal from a pair of NIRS channel during a 6 minute run (A), examples of individual motion artifacts (B, C, D and E) as recorded from collodion-fixed fiber probe and Velcro probe at 690 nm.

NIH-PA Author Manuscript

NIH-PA Author Manuscript

NIH-PA Author Manuscript

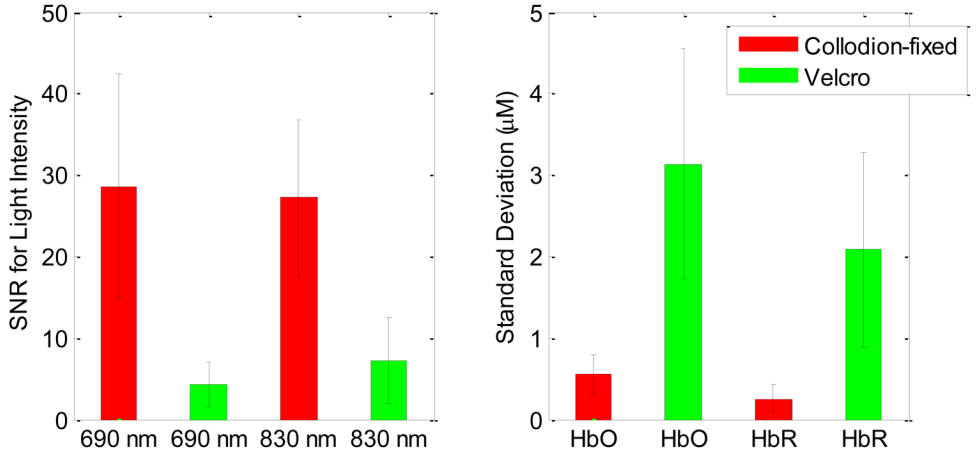

Fig. 5.

The mean and standard deviation of SNR values at 690 and 830 nm wavelengths averaged over five subjects (left), the mean and standard deviation of standard deviation of the changes in HbO and HbR averaged over five subjects (right) for collodion-fixed fiber probe and Velcro probe.

NIH-PA Author Manuscript

NIH-PA Author Manuscript

NIH-PA Author Manuscript

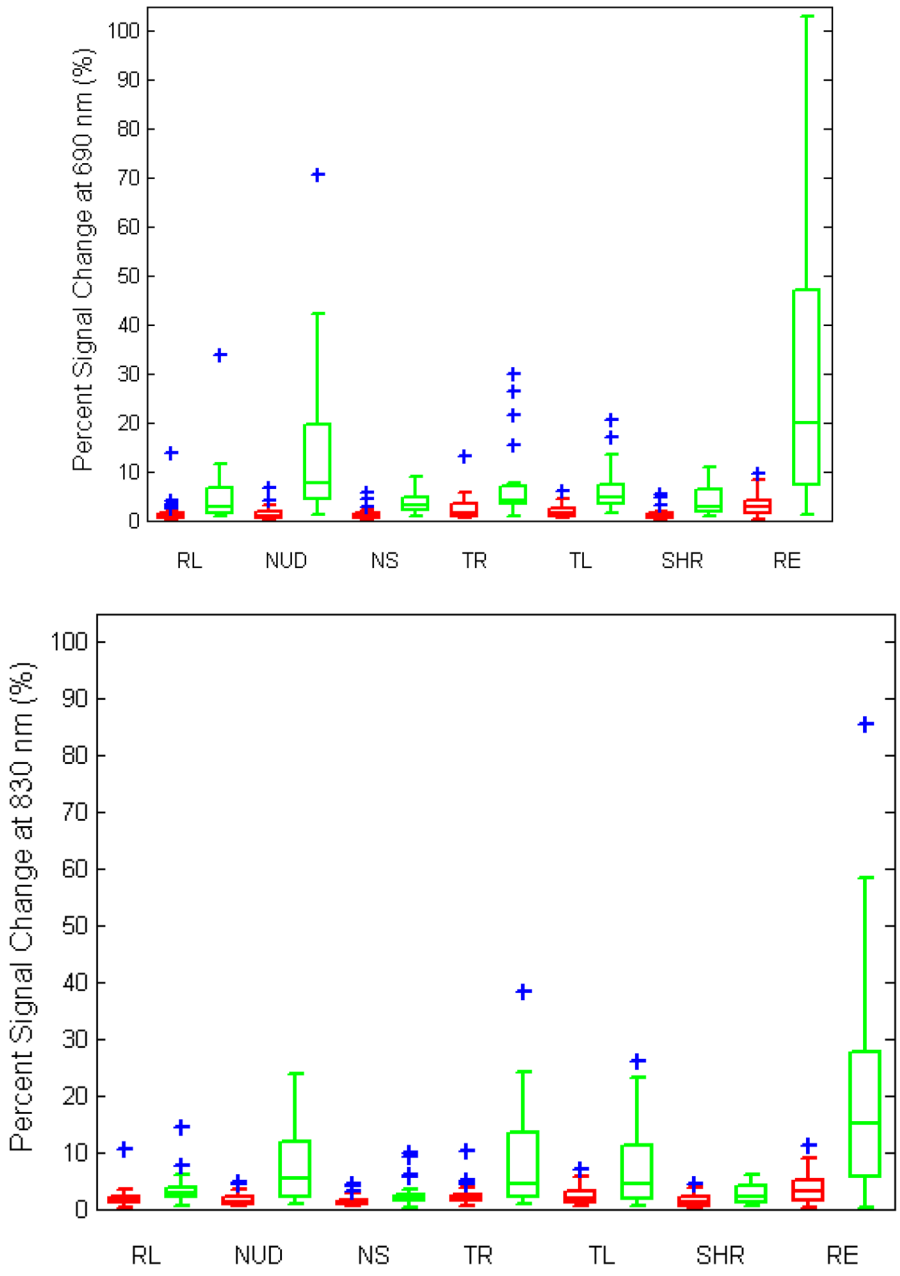

Fig. 6.

Percent signal change during motion artifact averaged over trials for collodion-fixed probes (red) and Velcro-probes (green) at 690 and 830 nm wavelengths. The central line shows the median, the edges of the box are the 25th and 75th percentiles and the blue plus signs are outliers. (RL: reading loudly, NUD: nodding up and down, NS: nodding sideways, TR: twisting right, TL: twisting left, SHR: shaking head rapidly, RE: raising eyebrows.)

NIH-PA Author Manuscript

NIH-PA Author Manuscript

NIH-PA Author Manuscript

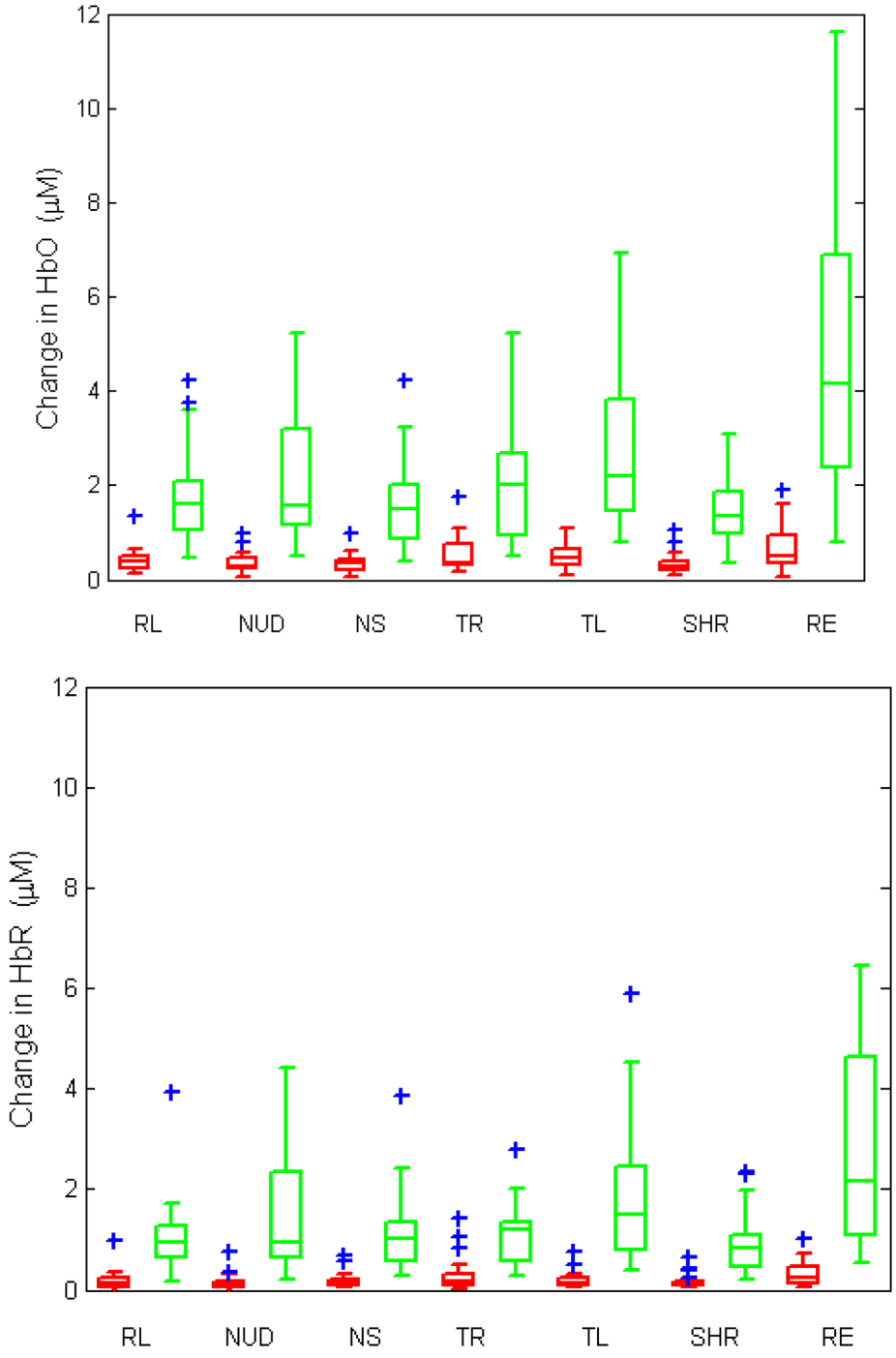

Fig. 7.

Changes in HbO and HbR (in molars) during motion artifact averaged over trials for collodion-fixed probes (red) and Velcro-probes (green). The central line shows the median, the edges of the box are the 25th and 75th percentiles and the blue plus signs are outliers. (RL: reading loudly, NUD: nodding up and down, NS: nodding sideways, TR: twisting right, TL: twisting left, SHR: shaking head rapidly, RE: raising eyebrows.)

NIH-PA Author Manuscript
NIH-PA Author Manuscript
NIH-PA Author Manuscript

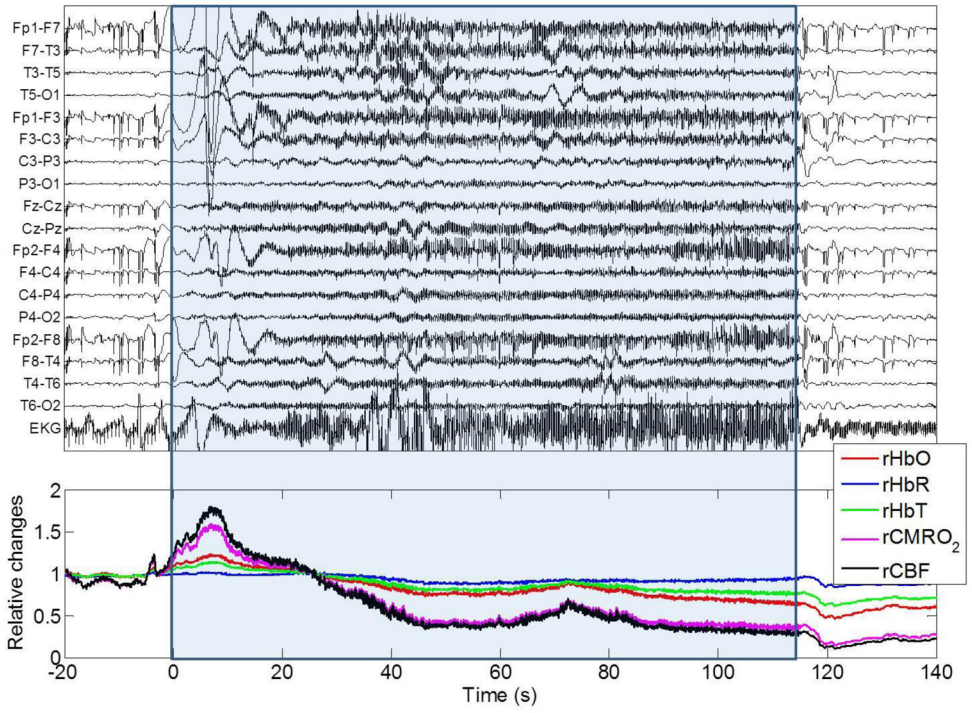

Fig. 8.

EEG trace and NIRS recordings during seizure 1 of Subject 1. The time zero is the start of the seizure as defined by clinical inspection of the EEG trace (performed by SC). rHbO: relative oxyhemoglobin, rHbR: relative deoxyhemoglobin, rtHb: relative total hemoglobin, $rCMRO_2$: relative cerebral metabolic rate of oxygen, rCBF: relative cerebral blood flow. (F: frontal, T: temporal, C: central, P: parietal, O: occipital, EKG: electrocardiogram). The blue box indicates the start and the end of the epileptic seizure determined from electrophysiology as well as patient video recordings by an epileptologist.

NIH-PA Author Manuscript

NIH-PA Author Manuscript

NIH-PA Author Manuscript

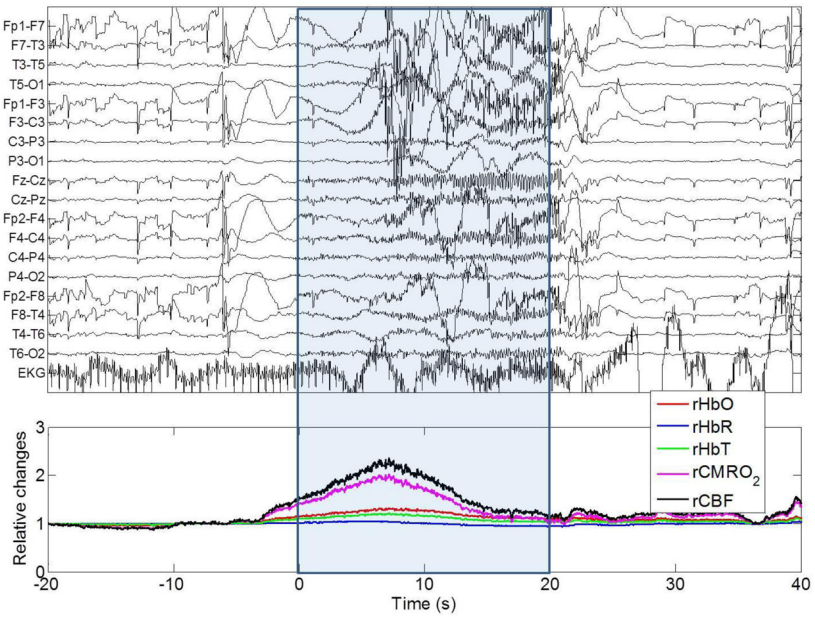

Fig. 9.

EEG trace and NIRS recordings during a seizure from Subject 1(7002). The time zero is the start of the seizure. rHbO: relative oxyhemoglobin, rHbR: relative deoxyhemoglobin, rtHb: relative total hemoglobin, $rCMRO_2$: relative cerebral metabolic rate of oxygen, rCBF: relative cerebral blood flow. (F: frontal, T: temporal, C: central, P: parietal, O: occipital, EKG: electrocardiogram). The blue box indicates the start and the end of the epileptic seizure determined from electrophysiology as well as patient video recordings by an epileptologist.

NIH-PA Author Manuscript

NIH-PA Author Manuscript

NIH-PA Author Manuscript

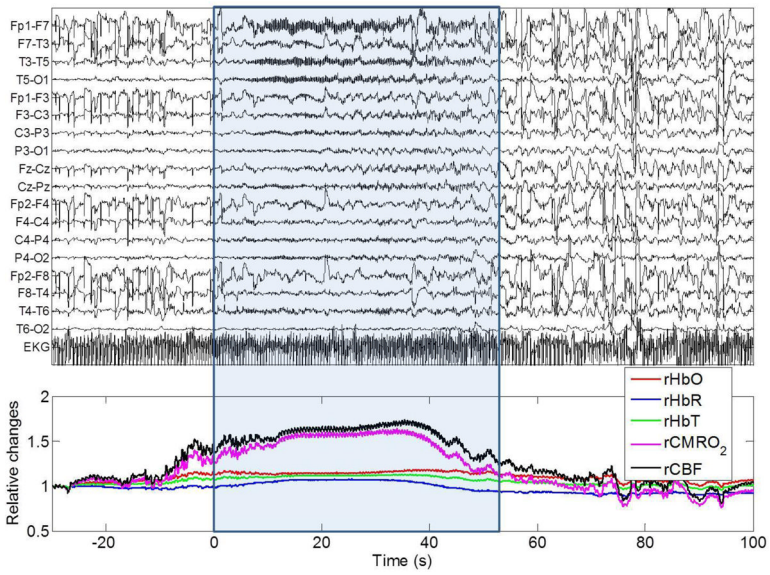

Fig. 10.

EEG trace and NIRS recordings during a seizure from Subject 2 (7004). The time zero is the start of the seizure. rHbO: relative oxyhemoglobin, rHbR: relative deoxyhemoglobin, rtHb: relative total hemoglobin, $rCMRO_2$: relative cerebral metabolic rate of oxygen, rCBF: relative cerebral blood flow. (F: frontal, T: temporal, C: central, P: parietal, O: occipital, EKG: electrocardiogram). The blue box indicates the start and the end of the epileptic seizure determined from electrophysiology as well as patient video recordings by an epileptologist.

NIH-PA Author Manuscript

NIH-PA Author Manuscript

NIH-PA Author Manuscript

Table 1

Subject information

	Focus	Age	Gender	Recording time
1	ultimately unclear, very likely right hemisphere in origin and probably right frontal	36	M	6 hrs
2	left temporal lobe (left mesial temporal sclerosis)	59	F	18 hrs

NIH-PA Author Manuscript

NIH-PA Author Manuscript

NIH-PA Author Manuscript

Table 2

Median percent signal changes for Velcro-probe and collodion-fixed probe at 690 and 830 nm wavelengths

	690 nm		830 nm	
	Collodion-fixed	**Velcro**	**Collodion-fixed**	**Velcro**
RL	1.0	2.7	1.4	2.6
NUD	0.8	7.5	1.2	5.4
NS	0.9	3.1	1.2	1.9
TR	1.6	3.9	2.2	4.4
TL	1.4	4.5	1.9	4.4
SHR	1.2	2.7	1.1	2.0
RE	2.9	19.9	2.9	14.9

NIH-PA Author Manuscript

NIH-PA Author Manuscript

NIH-PA Author Manuscript

Table 3

Median values of change in HbO and HbR for Velcro-probe and collodion-fixed probe (μM)

	HbO		HbR	
	Collodion-fixed	**Velcro**	**Collodion-fixed**	**Velcro**
RL	0.4	1.6	0.1	1.0
NUD	0.3	1.6	0.1	0.9
NS	0.3	1.5	0.1	1.0
TR	0.4	2.0	0.2	1.2
TL	0.5	2.2	0.1	1.5
SHR	0.3	1.4	0.1	0.8
RE	0.5	4.1	0.3	2,2